Stable Protein Device Platform Based on Pyridine Dicarboxylic Acid-Bound Cubic-Nanostructured Mesoporous Titania Films

Hwajeong Kim,[†,‡] Sung Soo Park,[§] Jooyeok Seo,[†] Chang-Sik Ha,*[,§] Cheil Moon,[⊥] and Youngkyoo Kim*[,†]

[†]Organic Nanoelectronics Laboratory, Department of Chemical Engineering, and [‡]Research Institute of Advanced Energy Technology, Kyungpook National University, Daegu 702-701, Republic of Korea

[§]Department of Polymer Science and Engineering, Pusan National University, Busan 609-735, Republic of Korea

[⊥]Department of Brain Science, Daegu Gyeongbuk Institute of Science and Technology (DGIST), Daegu 711-873, Republic of Korea

Ⓢ Supporting Information

ABSTRACT: Here we shortly report a protein device platform that is extremely stable in a buffer condition similar to human bodies. The protein device platform was fabricated by covalently attaching cytochrome *c* (cyt *c*) protein molecules to organic coupler molecules (pyridine dicarboxylic acid, PDA) that were already covalently bound to an electron-transporting substrate. A cubic nanostructured mesoporous titania film was chosen as an electron-transporting substrate because of its large-sized cubic holes (~7 nm) and highly crystalline cubic titania walls (~0.4 nm lattice). Binding of PDA molecules to the mesoporous titania surface was achieved by esterification reaction between carboxylic acid groups (PDA) and hydroxyl groups (titania) in the presence of 1-ethyl-3-(3-dimethylaminopropyl) carbodiimide (EDC) mediator, whereas the immobilization of cyt *c* to the PDA coupler was carried out by the EDC-mediated amidation reaction between carboxylic acid groups (PDA) and amine groups (cyt *c*). Results showed that the 2,4-position isomer among several PDAs exhibited the highest oxidation and reduction peak currents. The cyt *c*-immobilized PDA-bound titania substrates showed stable and durable electrochemical performances upon continuous current−voltage cycling for 240 times (the final current change was less than 3%) and could detect superoxide that is a core indicator for various diseases including cancers.

KEYWORDS: protein device, cytochrome c, mesoporous titania, organic coupler, stability, superoxide
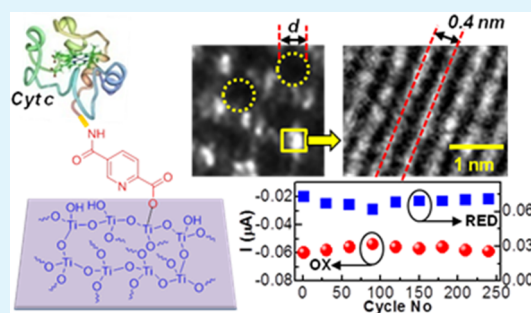
INTRODUCTION

Biomedical devices including biosensors and medical diagnostic devices have been extensively studied because we (humans) want to live longer and longer through overcoming fatal diseases by monitoring the disease symptoms at the early stage.[1−5] For practical applications to human, biomedical devices should be reliable and durable when they detect any chemicals or germs that are related with diseases.[6] Of various biomedical devices, particularly, proteins are widely used as active sensory parts because of their specific antigen−antibody interaction mechanisms.[7] In this regard, great efforts have been attempted to achieve stable biomedical devices which contain protein molecules in the sensory units.[8−10]

Cytochrome *c* (cyt *c*) is a typical protein that can detect superoxide (O_2^-) and nitric oxide (NO), which give signs for possible diseases such as cancer, diabetes, Alzheimer's disease, and Parkinson's disease.[11,12] The most widely used principle of cyt *c*−based devices is to monitor the electron transfer when the cyt *c* molecules undergo oxidation and reduction processes upon specific interaction with external molecules. Hence, the stable binding between cyt *c* molecules and electrodes is of importance to acquire reliable signals during the interaction (detection) process.

To date, two most reasonable methods to bind the cyt *c* molecules on the electrodes have been reported: (1) binding by coating of the mixtures of cyt *c* molecules and polymeric binders on the electrode surface because this method is simple and cost-effective,[13] (2) binding by charge interaction between cyt *c* molecules and electrode surfaces because the cyt *c* molecules have polar groups such as amine (−NH₂), carboxylic acid (−COOH), and amide bonds (−CONH−).[14,15] However, these approaches deliver a minimal binding state (i.e., physical adhesion) but cannot bestow a fundamentally strong bonding (i.e., covalent bond).

Hence, in this work, we attempted to bind the cyt *c* molecules on the electrode surface by employing an organic coupler (pyridine dicarboxylic acid, PDA) for better immobilization of cyt *c* molecules via an anchoring role of the PDA coupler (see Figure 1a). Four different PDA isomers, pyridine-2,4-dicarboxylic acid (P-2,4-DA), pyridine-2,5-dicarboxylic acid (P-2,5-DA), pyridine-2,6-dicarboxylic acid (P-2,6-DA), and pyridine-3,5-dicarboxylic acid (P-3,5-DA), were tried to
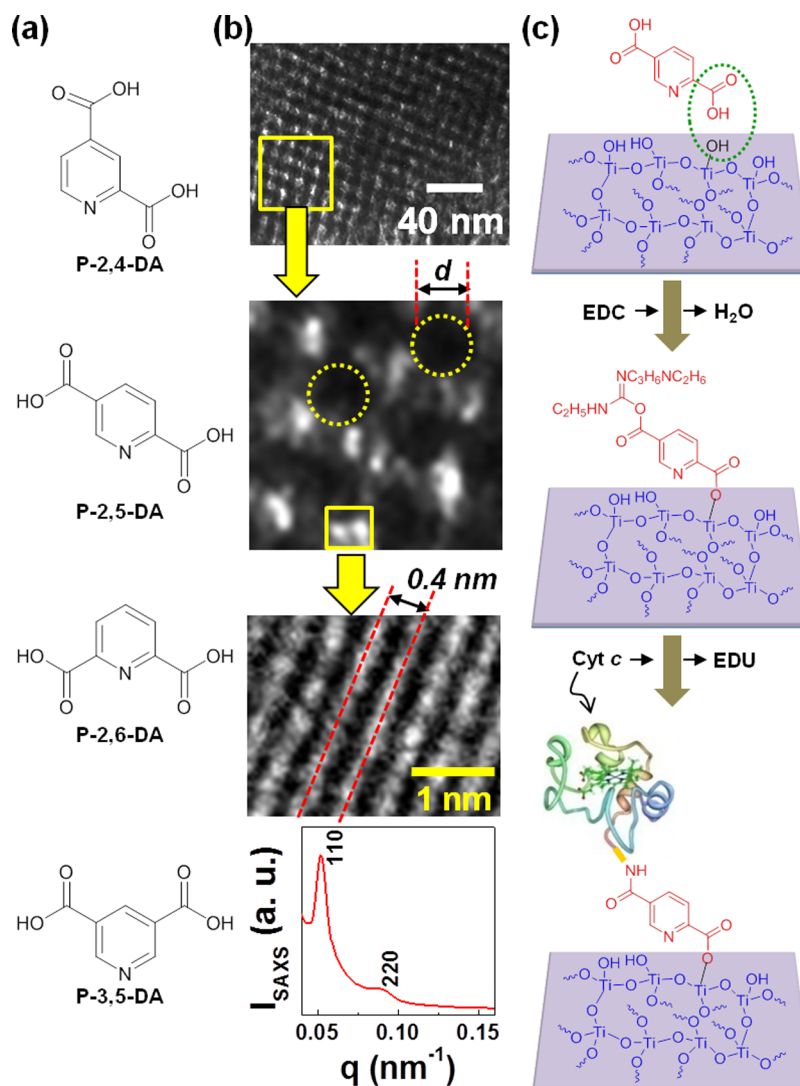
Figure 1. (a) Chemical structure of PDA (the number in the PDA denotes the position of dicarboxylic acids), (b) TEM images and SAXS profile (bottom) of mesoporous titania (MT) films (d = 7.3 nm), and (c) illustration for the reactions of PDA-MT and PDA-cyt c (cyt c size ≈ 3.4 nm).

investigate any position influence of two carboxylic acid groups in the PDA molecules. As an electron-accepting electrode media, a titanium oxide (titania - TiO_2) interlayer was introduced because the titania surface possesses abundant hydroxyl groups (−OH) suitable for the esterification reaction with the carboxylic acid groups in the PDA coupler molecules and crystalline titania films feature considerably high electron mobility (conductivity).[16,17] In particular, the present titania films were prepared to have mesoporous cubic nanostructures in order to maximize the area of titania surfaces where the cyt c molecules bind covalently. Here we note that PDA and titania are well-matched because a pyridine ring has an electron-deficient structure (an electron acceptor) so that it can keep the nature of electron-accepting nature of titania.[18,19]

■ RESULTS AND DISCUSSION

As shown in Figure 1b, a well-organized mesoporous cubic nanostructure ($m3m$; d-spacing = 12.08 nm; unit cell parameter (a) = 13.95 nm from the SAXS profile)[20] was measured from the mesoporous titania (MT) films that were coated on the ITO-glass substrates. The size of cubic holes was approximately 7.3 nm, whereas the crystal lattice of the titania walls was well

aligned with the lattice spacing of ca. 0.4 nm. By the esterification reaction aided by the coupling agent (1-ethyl-3-(3-dimethylaminopropyl) carbodiimide, EDC),[21] the PDA couplers were covalently bound to the surface of the MT films, followed by the amidation reaction of cyt c molecules to the unreacted carboxylic acid groups in the PDA molecules that are bound to the MT films (see Figure 1c). Here considerable amount of cyt c molecules are expected to be inserted into the cubic holes in the MT films because one or two cyt c molecules could be inserted into each cubic hole when it comes to the molecular size of cyt c (~3.4 nm).[22]
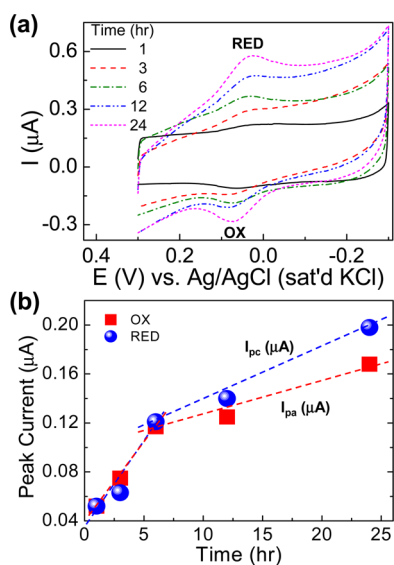
The esterification reaction of PDA to the MT surface was characterized by the shift of titania (Ti−O) O1s XPS spectra toward lower energy region owing to the reduced polarity by the presence of the ester group (Ti−O−C═O) instead of Ti−OH group (Figure 2a).[23] This was confirmed again from the formation of N1s XPS peak (C−N bond in a pyridine ring) in the case of the PDA-bound MT films (Figure 2b), whereas the amide N1s XPS peak (cyt c) was found at a higher binding energy region for the cyt c-immobilized PDA-bound MT film.[24] The additional evidence were also provided from the C1s XPS
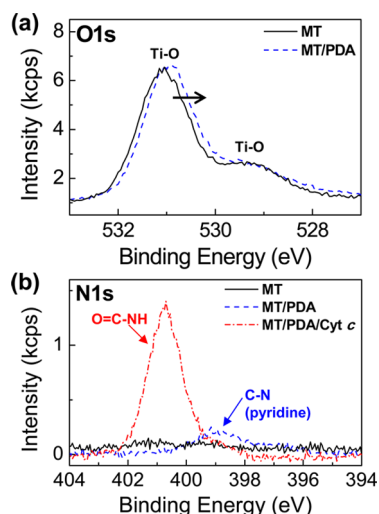
Figure 2. (a) O1s XPS spectra of the mesoporous titania (MT) film-coated on ITO-glass substrate and the PDA-bound MT film (MT/PDA), (b) N1s XPS spectra of the MT film-coated on ITO-glass substrate and the PDA-bound MT film and cyt c-immobilized PDA-bound MT film (MT/PDA/cyt c).

peaks for the reaction of PDA-MT and PDA-cyt c (see Figure S1 in the Supporting Information).

The immobilization reaction of cyt c to the PDA coupler that is bound to the MT films was initialized at 25 °C for 4 h and then completed at 4 °C for additional 24 h (see details in the Materials and Methods section). The additional immobilization time (24 h) was determined from a brief experiment by changing the storage time of the PDA-bound MT film samples in a 5 mM phosphate buffer solution (pH 7.4) with 50 mM cyt c at 4 °C (note that we used P-2,4-DA for this experiment). As shown Figure 3a, both reduction and oxidation peaks of cyt c

were gradually increased in the presence of marginal change of ΔE_p as the storage time increased from 1 to 24 h. Interestingly, both oxidation peak current (I_{pa}) and reduction peak current (I_{pa}) were relatively steeply increased up to 6 h and then exhibited a slower slope up to 24 h (see Figure 3b and Table 1).

Table 1. Summary of Oxidation Peak Current (I_{pa}) and Potential (E_{pa}), Reduction Peak Current (I_{pc}) and Potential (E_{pc}), and Redox Peak Potential Difference (ΔE_p) According to Immobilization Time of cyt c on P-2,4-DA Molecules

time (h)	I_{pa} (μA)	I_{pc} (μA)	E_{pa} (mV)	E_{pc} (mV)	ΔE_p (mV)
1	0.052	0.052	68	43	25
3	0.075	0.063	79	39	40
6	0.117	0.121	71	43	28
12	0.125	0.140	79	39	40
24	0.168	0.198	71	39	32

The reduction and oxidation peak current was increased by ~280% and ~220% by storing for 24 h at 4 °C, compared to the peak intensity at 1 h. This result implies that the cyt c molecules were continuously reacted to the PDA-bound MT film at this storage condition though the immobilization speed was changed at around 6 h. So 24 h was chosen for the present case because further increasing the storage time might increase more immobilization of cyt c but an unexpected deactivation of cyt c by immersing for longer time could be expected.

By employing above immobilization conditions, we carried out the cyt c immobilization reactions for all samples with different PDA isomers. As shown in Figure 4a, these samples
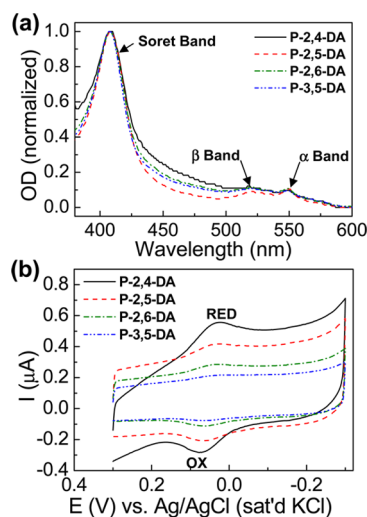
Figure 4. (a) Optical absorption spectra of the cyt c-immobilized PDA-bound MT films according to four different PDA isomers. (b) Cyclic voltammograms (CV) of the cyt c-immobilized PDA-bound MT films according to four different PDA isomers (OX: oxidation, RED: reduction): The CV measurement was carried out in the 0.2 M phosphate buffer solution (pH 7.4) at a scan rate of 50 mV/s.

Figure 3. (a) Cyclic voltammograms (CV) according to the storage time at 4 °C after initializing the immobilization reaction (4 h at 25 °C) of cyt c on the P-2,4-DA-bound MT films in a 5 mM phosphate buffer solution (pH 7.4) with 50 mM cyt c (OX: oxidation, RED: reduction). (b) Oxidation peak current (I_{pa}) and reduction peak current (I_{pc}) as a function of storage time. CVs were measured in the 0.2 M phosphate buffer solution (pH 7.4) at a scan rate of 50 mV/s.

showed three characteristic optical absorption peaks of cyt c such as Soret band, β band, and α band. This result indicates that all PDA isomers have a capability of immobilizing cyt c molecules in the presence of possible variations in terms of immobilized cyt c populations. Here it is noteworthy that the characteristic cyt c absorption peaks were measured for all samples irrespective of the PDA isomers, even though no cyt c

peaks were measured for the control sample (MT-coated ITO-glass substrates) that was cleaned (washed) after immersing in the same cyt *c* solution as for the immobilization reaction between cyt *c* and PDA-bound MT samples (see Figure S2 in the Supporting Information). In particular, considering the cyclic voltammetry (CV) curves of the cyt *c*-immobilized PDA-bound MT samples (Figure 4b), the 2,4-position PDA isomer (P-2,4-DA) seems to be more efficient than other isomers for the cyt *c* immobilization (note that the same CV measurement condition was applied for all samples). However, other samples also exhibited noticeable oxidation and reduction peaks, implying that other PDA isomers are also a promising potential candidate as a coupler if further optimization is followed. The resulting electrochemical parameters are summarized in Table 2

Table 2. Summary of Oxidation Peak Current (I_{pa}) and Potential (E_{pa}), Reduction Peak Current (I_{pc}), and Potential (E_{pc}), and redox peak potential difference (ΔE_p) According to the Position of Carboxylic Acids in the PDA Isomers

| coupler	I_{pa} (μA)	I_{pc} (μA)	E_{pa} (mV)	E_{pc} (mV)	ΔE_p (mV)
P-2,4-DA	0.198	0.168	71	39	32
P-2,5-DA	0.090	0.100	64	39	25
P-2,6-DA	0.073	0.060	68	39	29
P-3,5-DA	0.079	0.082	61	37	24

(see Figures S3 and S4 in the Supporting Information) for CV curves for control experiments). A particular attention can be paid to the small potential gap between oxidation and reduction peaks (ΔE_p = 24−32 mV), which indicates excellent electrochemical reversibility due to the stable binding of cyt *c* by the presence of PDA couplers.[25] Considering the fact that the ΔE_p values do not reflect the amount of cyt c immobilized (that is related to the redox peak current intensity),[14] the different ΔE_p values according to the different PDA isomers can be attributed to the different orientations (or positioning) of cyt *c* molecules because of the chemical structures of PDA isomers, though further separate study is required for confirmation.

To examine the stability (durability) of the present cyt *c*-immobilized PDA-bound MT samples, we measured the CV curves continuously up to 240 cycles. As shown in Figure 5a, the shape of CV curves was well maintained upon cycling in the presence of marginal variations. For more detailed investigation, the intensity of oxidation and reduction current peaks was plotted as a function of the cycle number. As shown in Figure 5b, the oxidation peak intensity was changed by ~10% at 90 cycles, whereas ~15% change was measured for the reduction peak at the same cycle number. After this cycle number, the peaks were stabilized leading to less than 3% variation (1.7% for oxidation and 2.7% for reduction). We consider that such good stability can be attributed mainly to the formation of covalent bonds between cyt *c* molecules and MT surfaces by the PDA couplers in the presence of additional effects of nanoholes in the MT surfaces which can strictly bind the cyt *c* molecules though further confirmation is needed. This result confirms that the present PDA coupler indeed contributed to the stabilized immobilization of cyt *c* proteins and the PDA-bound MT substrates can be an important platform for durable biomedical devices.

Finally, the possibility of the present cyt *c*-immobilized PDA-bound MT films as a biomedical device was briefly examined through the detection test of superoxide (O_2^-) with them. As shown in Figure 6a, superoxide molecules were generated by
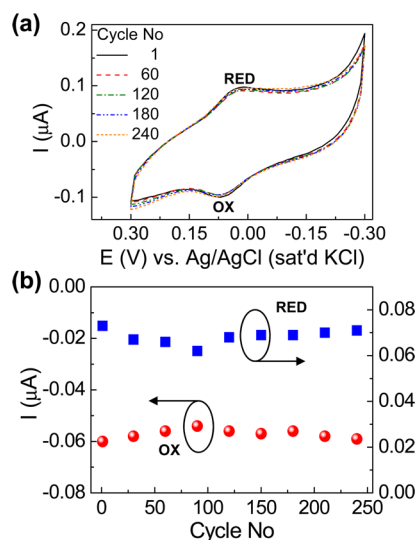
Figure 5. (a) Cyclic voltammograms (CV) of the cyt *c*-immobilized PDA-bound MT film (MT/PDA/cyt *c*) (only 5 curves are shown in order to avoid crowding data). (b) Current intensity variation of oxidation (OX) and reduction (RED) peaks in (a) as a function of cycle number: The CV measurement was carried out in the 0.2 M phosphate buffer solution (pH 7.4) at a scan rate of 50 mV/s.
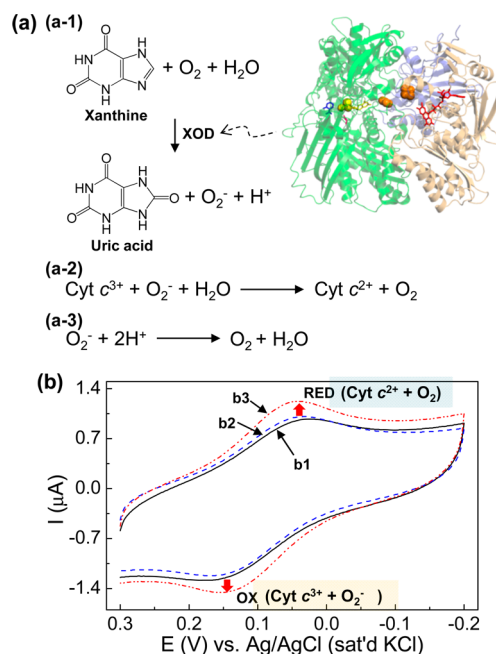
Figure 6. (a) Scheme for (a-1) superoxide (O_2^-) generation in the presence of xanthine and xantine oxidase (XOD) and (a-2 and a-3) reactions between cyt *c* and superoxide. (b) Cyclic voltammograms (CV) of the cyt *c*-immobilized P-2,4-DA-bound MT film (MT/P-2,4-DA/cyt *c*): (b1) without both xanthine and XOD, (b2) with xanthine, and (b3) with both xanthine and XOD (OX, oxidation; RED, reduction). The CV measurement was carried out in the 0.2 M phosphate buffer solution (pH 7.4) at a scan rate of 50 mV/s.

adding xanthine oxidase (XOD) to a buffer solution (0.2 M PBS, pH 7.4) with xanthine molecules in the presence of the cyt *c*-immobilized PDA-bound MT films.[26] According to the reaction scheme in Figure 6a, a pronounced redox current is expected by the reaction between the generated superoxide molecules and the cyt *c*-immobilized PDA-bound MT films. As

expected, a noticeably increased redox peak (~35% increment) was measured just in the case of the XOD-added solution, whereas no redox peak change was observed before adding the XOD molecules (see Figure 6b). Here we note that the redox peak in the cyt *c*-immobilized PDA-bound MT films was almost unchanged owing to no generation of superoxides after removing oxygen molecules by purging with nitrogen gas as shown in Figure S5 in the Supporting Information. This result supports that the present cyt *c*-immobilized PDA-bound MT films can be successfully used for the detection of superoxides that are one of key indicators for the diagnosis of cancers, diabetes, Alzheimer's disease, and Parkinson's disease.[11,12]

CONCLUSIONS

The stable protein (cyt *c*)-based platforms for biomedical devices were fabricated by employing an organic immobilization coupler (pyridine dicarboxylic acids - PDA). To enhance the immobilization yield and to secure the electron transport, cubic-nanostructured mesoporous titania (MT) films were introduced due to their relatively large-sized cubic holes (sufficient for the cyt *c* insertion) and highly crystalline titania walls (for better electron transport). The size of cubic holes prepared was ~7 nm, which can host about two cyt *c* molecules (theoretically), while the titania walls showed well-ordered crystalline nanostructure with a lattice distance of ~0.4 nm. The binding of PDA molecules to the titania surface was achieved by the EDC-mediated esterification between carboxylic acid groups (PDA) and hydroxyl groups (titania), which was confirmed by the XPS measurements. The immobilization of cyt *c* to the PDA coupler was carried out by the amidation reaction between carboxylic acid groups (PDA) and amine groups (cyt *c*). The 2,4-position PDA isomer showed the highest oxidation and reduction peak currents though the immobilization of cyt *c* molecules was successful for all PDA couplers used in this study. In particular, stable and durable electrochemical performances were measured for the present cyt *c*-immobilized PDA-bound MT substrates upon CV cycling for 240 times (the final current change was less than 3%). In terms of practical applications as a biomedical device, the present cyt *c*-immobilized PDA-bound MT substrates did successfully detect superoxides (O_2^-) that are generated in the circumstances of various diseases including cancers and Alzheimer's. Hence the present PDA coupler method is believed to provide a sustainable platform for sophisticated biomedical devices,[27] whereas its application range can cover a broad spectrum of organic and/or organic/inorganic hybrid devices for various applications.[28,29]

MATERIALS AND METHODS

Materials and Fabrication. Prior to coating the mesoporous titania (MT) layers, indium−tin oxide (ITO)-coated glass substrates (10 Ω/□) were cleaned with acetone and isopropyl alcohol, followed by drying with a nitrogen flow. On top of the cleaned ITO-glass substrates, a mixture solution (solvent = ethanol) of titania precursor ($TiCl_4$) and template polymer (Pluronic F-127) was coated and soft-baked at 130 °C for 24 h. These samples were subject to the calcination process for making mesoporous cubic titania nanostructure by removing the polymeric templates at 450 °C for 5 h under air flow condition (see Figure 1b). Then the samples were cleaned again with acetone and isopropyl alcohol to get rid of any organic contaminants remained during the calcination process. The cleaned MT-coated ITO-glass substrates were immersed in the solution that contains PDA molecules (30 mM) and 1-ethyl-3-(3-dimethylaminopropyl) carbodiimide (EDC, 70 mM) as a mediator. The esterification reaction

between hydroxyl groups (−OH) in MT and EDC-modified carboxylic acid groups (−COOH) in PDA was carried out at 30 °C for 8 h (see Figure 1c). Then the PDA-bound MT samples were cleaned in *N,N*-dimethylformamide (DMF) to remove any unreacted PDA molecules and remained EDC mediators. After cleaning, the PDA-bound MT-coated ITO-glass substrates were immersed in the cyt *c* solution (50 mM cyt *c* in 5 mM phosphate buffer solution: pH 7.4) for the amidation reaction of amine groups (−NH₂) in cyt *c* to the live EDC-modified carboxylic acid groups (−COOH) in the other side of the PDA molecules that are bound to the MT surfaces. This coupling (amidation) reaction was performed at 25 °C for 4 h: We note that 1-ethyl-3-(3-dimethylaminopropyl) urea (EDU) is released by the amidation reaction (see Figure 1). After amidation reaction, the cyt *c*-immobilized samples were stored at 4 °C for 24 h to complete immobilization step between cyt *c* and PDA molecules. The cyt *c*-immobilized samples were cleaned using 5 mM phosphate buffer solution (pH 7.4) and deionized water to remove cyt *c* molecules that are unreacted and physically adhered to the PDA-bound MT surfaces. To examine the possibility for practical biomedical devices, the cyt *c*-immobilized samples were immersed in 0.2 M phosphate buffer solution (PBS: pH 7.4) with 0.15 mM xanthine (Sigma-Aldrich), where superoxide (O_2^-) molecules are generated by adding 0.15 mM xanthine oxidase (XOD, Sigma-Aldrich).

Measurement. The nanostructure of MT films was examined with a high resolution transmission electron microscope (HRTEM, JEM-2010, JEOL), while the average pore size of the MT films was measured using a small-angle X-ray scattering (SAXS) system at Pohang Accelerator Laboratory (PAL, POSTECH, Korea) with CuKα (λ = 1.608 Å) radiation. The reaction between PDA (−COOH) and MT (−OH) by the aid of the EDC mediator was characterized with X-ray photoelectron spectroscopy (XPS, ESCALAB 250, VG Scientifics). The electrochemical characteristics and superoxide (O_2^-) detection of the cyt *c*-immobilized samples were measured in a 0.2 M phosphate buffer solution (pH 7.4) at a scan rate of 50 mV/s using a potentiostat (263A, Princeton Applied Research): we note that xanthine and XOD were added to the buffer solution for the superoxide detection experiment. The ITO-coated glass was used as a working electrode, while Ag/AgCl (sat'd KCl) and Pt wire were used as a reference electrode and a counter electrode, respectively. For the stability examination the cyclic voltammetry (CV) curves were continuously measured for the cyt *c*-immobilized samples that were loaded in the 0.2 M phosphate buffer solution (pH 7.4) upon cycling for 240 times using the same potentiostat.

ASSOCIATED CONTENT

Ⓢ Supporting Information
(1) XPS spectra, (2) optical absorption spectra, (3) CV curves of ITO/MT, ITO/MT/P-2,4-DA, and ITO/MT/P-2,4-DA/cyt *c*, (4) CV curves of cyt *c*-immobilized PDA-bound MT film (MT/PDA/cyt *c*) in a 0.2 M phosphate buffer solution (PBS: pH 7.4), and (5) CV curves of cyt *c*-immobilized P-2,4-DA-bound MT film (MT/P-2,4-DA/cyt *c*) in a nitrogen purged 0.2 M PBS (pH 7.4) solution with xanthine and XOD. This information is available free of charge via the Internet at http://pubs.acs.org.

AUTHOR INFORMATION

Corresponding Author
*E-mail: csha@pusan.ac.k (C.-S.H.), ykimm@knu.ac.kr (Y.K.). Tel: +82-53-950-5616.

Notes
The authors declare no competing financial interest.

ACKNOWLEDGMENTS

■ REFERENCES

(1) Perfézou, M.; Turner, A.; Merkoçi, A. *Chem. Soc. Rev.* **2012**, *41*, 2606−2622.

(2) Chen, W.; Cai, S.; Ren, Q.-Q.; Wen, W.; Zhao, Y.-D. *Analyst* **2012**, *137*, 49−58.

(3) Justino, C. I. L.; Rocha-Santos, T. A.; Duarte, A. C. *Trend. Anal. Chem.* **2010**, *29*, 1172−1183.

(4) Healy, D. A.; Hayes, C. J.; Leonard, P.; Mckenna, L. *Trend. Biotechnol.* **2007**, *25*, 125−131.

(5) Perry, M.; Li, Q.; Kennedy, R. T. *Anal. Chim. Acta* **2009**, *653*, 1−22.

(6) Eggins, B. R. *Chemical Sensors and Biosensors*; John Wiley & Sons, New York, 2002.

(7) Conroy, P. J.; Hearty, S.; Leonard, P.; O'Kennedy, R. J. *Semin. Cell Dev. Biol.* **2009**, *20*, 10−26.

(8) Scouten, W. H.; Luong, J. H. T.; Brown, R. S. *Trend. Biotechnol.* **1995**, *13*, 178−185.

(9) Ronkainen, N. J.; Halsall, H. B.; Heineman, W. R. *Chem. Soc. Rev.* **2010**, *39*, 1747−1763.

(10) Nam, S.; Kim, H.; Kim, Y. *Nanoscale* **2010**, *2*, 694−696.

(11) Rahimi, P.; Ghourchian, H.; Rafiee-Pour, H.-A. *Analyst* **2011**, *136*, 3803−3803.

(12) Bedioui, F.; Quinton, D.; Griveau, S.; Nyokong, T. *Phys. Chem. Chem. Phys.* **2010**, *12*, 9976−9988.

(13) Wael, K. D.; Bashir, Q.; Vlierberghe, S. V.; Dubruel, P.; Heering, H. A.; Adriaens, A. *Bioelectrochemistry* **2012**, *83*, 15−18.

(14) Fedurco, M. *Coord. Chem. Rev.* **2000**, *209*, 263−331.

(15) Topoglidis, E.; Campbell, C. J.; Cass, A. E. G.; Durrant, J. R. *Langmuir* **2001**, *17*, 7899−7906.

(16) Snaith, H. J.; Grätzel, M. *Adv. Mater.* **2007**, *19*, 3643−3647.

(17) Hendry, E.; Wang, F.; Shan, J.; Heinz, T. F.; Bonn, M. *Phys. Rev. B* **2004**, *69*, 081101(1)−081101(4).

(18) Grätzel, M. *Nature* **2001**, *414*, 338−344.

(19) Hagfel, A.; Boschloo, G.; Sun, L.; Kloo, L.; Pettersson, H. *Chem. Rev.* **2010**, *110*, 6595−6663.

(20) Crepaldi, E. L.; Soler-Illia, G. J. de A. A.; Grosso, D.; Cagnol, F.; Ribot, F.; Sanchez, C. *J. Am. Chem. Soc.* **2003**, *125*, 9770.

(21) Gao, J.; Cui, Y.; Yu, J.; Lin, W.; Wang, Z.; Qian, G. *J. Mater. Chem.* **2011**, *21*, 3197−3203.

(22) Kim, H.; Degenaar, P.; Kim, Y. *J. Phys. Chem. C* **2009**, *113*, 14377−14380.

(23) Pouilleau, J.; Devilliers, D.; Groult, H.; Marcus, P. *J. Mater. Sci.* **1997**, *32*, 5645−5651.

(24) Song, S.; Clark, R. A.; Bowden, E. F.; Tarlov, M. J. *J. Phys. Chem.* **1993**, *97*, 6564−6572.

(25) Bard, A. J.; Faulkner, L. R. *Electrochemical Methods: Fundamentals and Applications*, 2nd ed.; John Wiley & Sons: New York, 2001.

(26) Lvovich, V.; Scheeline, A. *Anal. Chem.* **1997**, *69*, 454−462.

(27) Kim, H.; Kim, S. Y.; Nam, S.; Ronnett, G. V.; Han, H. S.; Moon, C.; Kim, Y. *Analyst* **2012**, *137*, 2047−2053.

(28) Nam, S.; Shin, M.; Kim, H.; Ha, C. S.; Ree, M.; Kim, Y. *Adv. Funct. Mater.* **2011**, *21*, 4527−4534.

(29) Nam, S.; Kim, J.; Lee, H.; Kim, H.; Ha, C. S.; Kim, Y. *ACS Appl. Mater. Interfaces* **2012**, *4*, 1281−1288.